Investigation of Nanostructure and Properties of Aromatic–Aliphatic Polyamide-Based Nanocomposites with Clay Additives

Sonia Zulfiqar,[1,2] Saima Shabbir,[1] Muhammad Ishaq,[1] Muhammad Ilyas Sarwar[1,2]

[1]*Department of Chemistry, Quaid-i-Azam University, Islamabad-45320, Pakistan*
[2]*Department of Materials Science and Engineering, University of Delaware, Newark, Delaware 19716*

Received 20 March 2008; accepted 11 November 2008
DOI 10.1002/app.29714
Published online 25 February 2009 in Wiley InterScience (www.interscience.wiley.com).

ABSTRACT: Aromatic–aliphatic polyamide/clay nanocomposites were produced using solution intercalation technique. Surface modification of the clay was performed with ammonium salt of aromatic diamine and the polyamide chains were produced by condensation of 4-aminophenyl sulfone with sebacoyl chloride (SCC) in dimethyl acetamide. Carbonyl chloride endcapped polymer chains were prepared by adding extra SCC near the end of polymerization reaction. The nanocomposites were investigated for organoclay dispersion, water absorption, mechanical, and thermal properties. Formation of delaminated and intercalated nanostructures was confirmed by X-ray diffraction and TEM studies. Tensile strength and modulus improved for nanocomposites with optimum organoclay content (8 wt %). Thermal stability and glass transition temperatures of nanocomposites increased relative to pristine polyamide with augmenting organoclay content. The amount of water uptake for these materials decreased as compared with the neat polyamide. J Appl Polym Sci 112: 3141–3148, 2009

Key words: polyamides; organoclay; nanocomposites; morphology; mechanical properties; thermal properties

INTRODUCTION

Polymer–clay composites have attracted much interest because incorporation of clay into polymers at the nanoscale yield improved mechanical, thermal, flammability, and other properties at low clay contents (<10 wt %).[1] These materials have been prepared in different ways: intercalation in solution,[2] *in situ* polymerization,[3] and direct melt intercalation.[4] The replacement of exchangeable inorganic cations in the interlayer spacings of the native clay by cationic surfactants such as alkyl/aryl ammonium ions is known to compatibilize the surface chemistry of the clay and hydrophobic polymer matrix. The role of ammonium cations in the organosilicate is to lower the surface energy of the inorganic filler and improve its wetting characteristics with the polymer host. Additionally, organic cations may provide various functional groups that can react with the polymer to improve adhesion. Generally, two main types of composites (intercalated and delaminated structures) may be obtained when layered silicates are associated with different polymer matrices, such as polyamides,[5–16] polystyrene,[17–22] polypropylene,[23–26] polyethylene,[27,28] Poly(methyl methacrylate) [PMMA],[29,30] Poly(ethylene oxide) [PEO],[31,32] epoxy polymer, and others.[33–37] These primarily depend on the method of preparation and the nature of components used (layered silicate, organic cation, and polymer matrix). Organic surfactants such as quaternary ammonium salts of aliphatic/aromatic amines and various silicon–organic reagents are used to have good morphology and nanostructure.

Polyamides are recognized for their outstanding properties in terms of thermal stability, mechanical properties, high glass transition temperature, and good resistance to solvents. The aromatic polyamides because of their high performance and superb properties are widely utilized for aerospace applications.[38–43] The aliphatic polyamides generally referred to as nylons are used in many daily life applications. Glassy copolymer obtained from the condensation of aromatic diacids and aliphatic diamines comprises another type of polyamides often known as glass-clear nylons with excellent properties such as good transparency, rigidity, thermal resistance, hardness, etc. and have many industrial applications. The important commercial examples of these materials are Trogamid T®, Grilamid TR-55®, and Hostamid

Correspondence to: M. I. Sarwar (ilyassarwar@hotmail.com).

Contract grant sponsor: Higher Education Commission of Pakistan (HEC); contract grant number: 20-23-ACAD (R) 03-410.

LP700®, which are the combinations of diacids with mixture of different diamines. If the aromatic diacid is polycondensed with a 1 : 1 mixture of 2,2,4- and 2,4,4-trimethylhexa-methylene diamine, a transparent and high melting temperature polyamide is obtained which is commonly known as Trogamid®. It has excellent properties e.g., good transparency and rigidity, greater hardness, low temperature coefficient of expansion, good thermal resistance and insulation properties and has many industrial applications. The mechanical properties of these materials can further be improved by introducing the ceramic phases.[44–46]

In this attempt, we have focused on the nanocomposites of organoclay with soluble aromatic–aliphatic polyamide prepared through solution intercalation technique. The polyamide chains were produced by reacting 4-aminophenylsulfone with SCC in anhydrous *N*,*N*′-dimethyl acetamide (DMAc). The amide chains were modified with carbonyl chloride groups using 1% excess diacid chloride. Montmorillonite (MMT) was converted into organophilic using aromatic diamine in such a way that modified ammonium cation attached to the negatively charged silicate layers by replacing the metal cation, whereas the other free amino group of the diamine could interact with carbonyl chloride end-capped polyamide diffused into the space between the silicate layers. As a result, chemically combined and thermally more stable nanocomposites were produced with permanent intercalating effect. Thin nanocomposite films obtained by evaporation of the solvent were subjected for XRD, TEM, and mechanical testing: TGA, DSC, and water uptake measurements.

EXPERIMENTAL

Materials

4-Aminophenyl sulfone (APS) 97%, SCC 97%, MMT K-10 (cation exchange capacity of 119 mequiv/100 g), *p*-phenylene diamine (*p*-PDA) >99%, silver nitrate (99.9%), and DMAc >99% (dried over molecular sieves before use) were obtained by the courtesy of Aldrich (Germany) and used as received. Triethylamine (TEA) ≥99.5% and hydrochloric acid (37%) procured from Fluka (Switzerland) were used as such.

Synthesis of aromatic–aliphatic polyamide matrix

Aromatic–aliphatic polyamide was synthesized by low-temperature polycondensation method from the aromatic diamine and aliphatic diacid chloride. In a typical reaction, 0.05 mol 4-aminophenylsulfone and 100 mL DMAc were taken in a flask equipped with a magnet stirrer under anhydrous conditions. The diamine was dissolved for 30 min. Then 0.05 mol of SCC was added and the reaction mixture was agitated at 0°C for 1 h to avoid the heat produced during the polymerization reaction. The temperature was raised to room temperature and the solution was agitated for 24 h to ensure completion of the reaction. To produce carbonyl chloride chain ends, 1% diacid chloride was added to the reaction mixture. The polymer formed was viscous and golden in color (Scheme 1). A stochiometric amount of TEA was added after acyl chloride to remove HCl produced during the polymerization reaction otherwise it would act as an impurity that might yield a low molecular weight polymer. The solution was centrifuged to isolate the precipitates from the neat polyamide. The prepared polymer resin served as a stock solution for nanocomposite formation.

Preparation of *p*-PDA-MMT

Organo-MMT was prepared by cationic exchange between the inorganic cations in the MMT interlayers and ammonium cations of *p*-PDA in an aqueous solution (Scheme 2). Cations of swelling agent were prepared by dropwise addition of HCl in the *p*-PDA solution in water with heating at 80°C. MMT was suspended in distilled water at 80°C. The suspension of layered silicates was mixed with cationic solution of *p*-PDA with vigorous stirring for 3 h at 60°C. The precipitates of organoclay were isolated, washed with hot water thrice, and then filtered to remove the residual amount of the cationic salt. The removal of

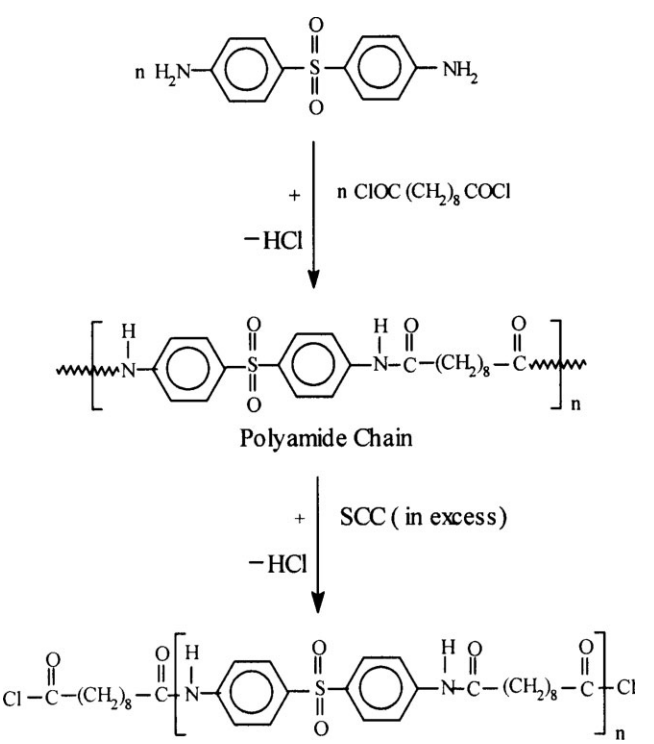

Scheme 1 Formation of carbonyl chloride end-capped aromatic–aliphatic polyamide chains.

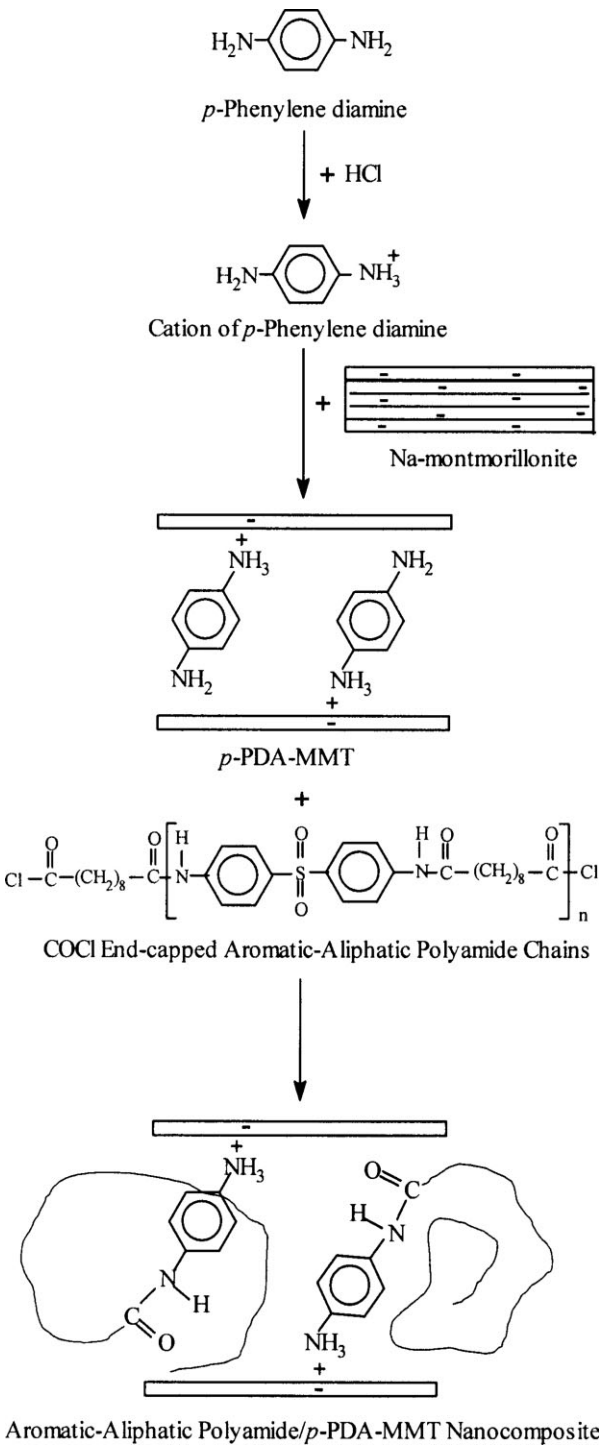

Scheme 2 Schematic representation for the formation of aromatic–aliphatic polyamide nanocomposites with *p*-PDA-MMT.

chloride ions was verified by the titration of filtrate with $AgNO_3$ until no AgCl precipitates appeared. The final product obtained by filtration was dried in vacuum at 60°C for 24 h. The dried cake was ground and screened with a 325-mesh sieve. The modified clay labeled as *p*-PDA-MMT was used for the preparation of nanocomposites.

Synthesis of polyamide/*p*-PDA-MMT nanocomposites

Nanocomposites were prepared by solution mixing of the appropriate amounts of *p*-PDA-MMT and polyamide resin into 50 mL flask for a particular concentration. The mixture was stirred at a high speed for 24 h for good dispersion of organoclay in the polyamide matrix. Different compositions of the hybrid materials having 2 to 20 wt % organoclay were prepared as mentioned earlier (Scheme 2). Thin composite films were cast by pouring the mixture solution into petri dishes placed on a levelled surface. The solvent was evaporated at 70°C for 6 h and hybrid films were further dried at 80°C under vacuum to a constant weight.

Characterization

FT-IR data of thin polyamide film was recorded using Excalibur series FT-IR spectrometer, Model No. FTSW 3000MX (BIO-RAD). Weight-average (M_w) and number-average (M_n) molecular weights of polyamide was determined using a GPC equipped with Waters 515 pump. Absolute *N,N*-dimethylformamide (DMF) was used as an eluent monitored through a UV detector (UV S3702 at 270 nm) with a flow rate of 1.0 mL/min at 60°C. XRD analysis was carried out in the reflection mode using a Philips PW 1820 diffractometer. Nickel-filtered Cu Kα radiation (radiation wavelength, $\lambda = 0.154$ nm) was produced by a PW 1729 X-ray generator at an operating voltage of 40 kV and a current of 30 mA. XRD measurements were recorded between $2\theta = 2$–10° with a step size of 0.02° to monitor the change in interlayer spacing of these materials. The morphology of nanocomposites was investigated by recording images using FEI Tecnai F20 transmission electron microscope operated at an accelerating voltage of 200 kV. The nanocomposite films were first microtomed into 60 nm ultra thin sections with a diamond knife using Leica Ultracut UCT ultramicrotome. Tensile properties of the nanocomposites (rectangular strips) having dimensions ($\sim 14 \times 5.2$–6.8×0.22–0.42 mm) were measured according to DIN procedure 53455 having a crosshead speed of 5 mm/min at 25°C using Testometric Universal Testing Machine M350/500. An average value obtained from 5 to 7 different measurements in each case has been reported.

The thermal stability of nanocomposites was measured using a METTLER TOLEDO TGA/SDTA 851^e thermogravimetric analyzer using 1–5 mg of the sample in Al_2O_3 crucible heated from 25 to 800°C at a heating rate of 10°C/min under nitrogen atmosphere with a gas flow rate of 30 mL/min. Glass transition temperatures of composite materials were monitored using a METTLER TOLEDO DSC 822^e

differential scanning calorimeter by taking 5–10 mg of each sample encapsulated in aluminum pans and heated at a ramp rate of 10°C/min under nitrogen atmosphere. The water uptake of nanocomposites was measured under ASTM D570-81 procedure in which the films were completely dried in vacuum and then weighed out for initial weight (W_o). The films were soaked in deionized water at 25°C for 24 h and then were taken out; washed gently to remove the excess water and weighed again. The process was repeated for further water uptake till the films almost attained a constant weight. The total soaking time was 168 h and the samples were weighed at regular 24 h time intervals to get the final weight (W_f). The percent increase in the weight of the samples was calculated using the formula $(W_f - W_o)/W_o$.

RESULTS AND DISCUSSION

The thin film obtained from polyamide was transparent and golden in color. The same film was used for structure elucidation and molecular weight determination of the neat polyamide. Various IR bands appeared in the spectrum are 3324 cm^{-1} (N—H stretching), 3100 cm^{-1} (aromatic C—H stretching), 2930 cm^{-1} and 2857 cm^{-1} (CH_2 asymmetric and symmetric stretching), 1681 cm^{-1} (C=O group), 1588 cm^{-1} (aromatic C=C stretching), 1315 cm^{-1} and 1152 cm^{-1} (S=O asymmetric and symmetric stretching). The IR data confirm the formation of the aromatic–aliphatic polyamide. The values of M_n, M_w, and polydispersity of polyamide were found to be 10133.10 g/mol, 20865.10 g/mol, and 2.06 respectively. The nanocomposite films with *p*-PDA-MMT containing up to 20 wt % organoclay were blackish grey in color and transparent at concentrations of organoclay up to 4 wt %. The color of films became darker with increase of *p*-PDA-MMT in the hybrids, and the films containing 12 wt % clay contents were semitransparent and became opaque on further loading of organoclay.

X-ray diffraction

XRD pattern of MMT, modified MMT, pure polymer resin, and nanocomposites are displayed in Figure 1. A normal diffraction peak around $2\theta = 8.78°$ equaling a *d*-spacing of 1.006 nm was observed for MMT. In case of *p*-PDA-MMT, a strong XRD peak at $2\theta = 5.94°$ indicates that layered silicate have been intercalated by *p*-PDA molecules to a *d*-spacing of 1.486 nm. The XRD curves of pure polyamide and composites containing up to 10 wt % *p*-PDA-MMT did not display

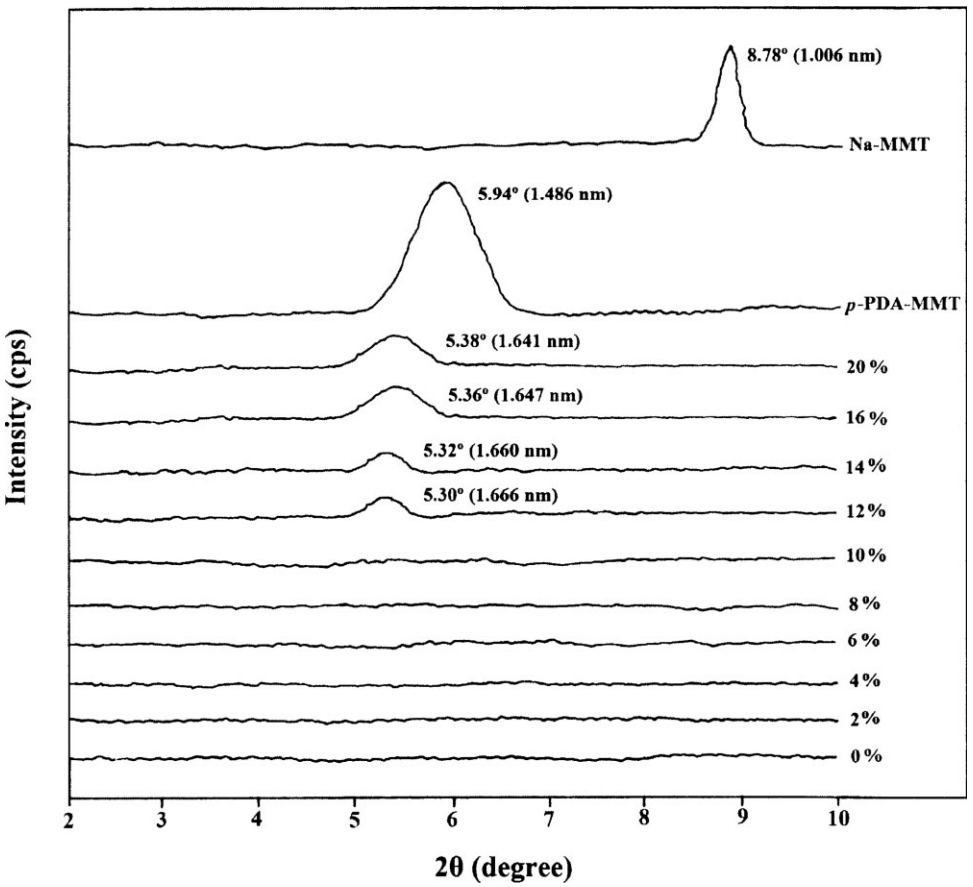

Figure 1 X-ray diffraction curves of aromatic–aliphatic polyamide/*p*-PDA-MMT nanocomposites.

Figure 2 TEM micrographs of aromatic–aliphatic polyamide-based nanocomposites containing (a) 4 wt %, (b) 10 wt %, and (c) 20 wt % *p*-PDA-MMT.

any diffraction peak in the 2θ range from 2 to 10°. This implies that *p*-PDA-MMT had been exfoliated in the nanocomposites. With 12 wt % organoclay, a small peak emerged at $2\theta = 5.30°$ (1.666 nm) predicting an intercalated morphology of the hybrid materials. The remaining high percentages of the nanocomposites showed a similar trend. When a polymer chain intercalates into the interlayers of clay, resulting in a finite gallery expansion, then polymer's transitional entropy increases whereas its conformational entropy decreases. At the same time, the modified clay gains conformational entropy. The formation of nanocomposites depends on both entropic and enthalpic contributions of the system, which are related to the properties of polymer and modified clay. Among them, the polarity of the polymer has greater effect on the enthalpic translation. Nonpolar polymers generally cannot insert into the interlayers of the clay.[47] The polyamide, being polar polymer, can make the enthalpic translation between the polymer and the modified clay much easier so that the chains of the polyamide can intercalate into the interlayers of the clay.

Transmission electron microscopy

A TEM analysis was carried out to harmonize the data obtained from XRD, because the latter generally fail to probe the disordered/exfoliated morphology (absence of diffraction peaks in XRD pattern) of the nanocomposites. The TEM images of various polyamide based hybrids are shown in Figure 2, where the dark lines represent silicate layers. The hybrid film containing 4 wt % clay content [Fig. 2(a)] shows well-dispersed clay platelets in the polyamide matrix. Although the Figure 2(b,c) represent the morphology of nanocomposites having 10 and 20 wt % *p*-PDA-MMT. These micrographs show regions with individual dispersion of partially delaminated sheets in the matrix and a regular stacking of sheets being maintained with a layer of polymer in between, which is consistent with the XRD results.

Mechanical properties

The tensile behavior of pure polyamide and nanocomposites containing various proportions of organoclay is shown in Figure 3 and the values are given in Table I. It is obvious from the figure that tensile strength of the composite materials has improved as compared with the neat polyamide. The maximum stress at break point increased initially and reached its maximum (27.5 MPa) at 8 wt % clay content, showing improvement in the tensile strength. However, with further addition of organoclay this value decreased. The length at break of nanocomposites also showed a

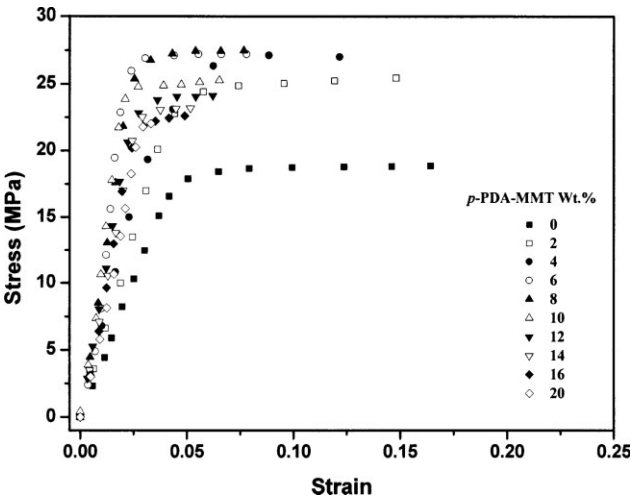

Figure 3 Stress–strain curves of aromatic–aliphatic polyamide/*p*-PDA-MMT nanocomposites.

decreasing behavior relative to the pure polyamide. The tensile modulus of pure polymer which was 386.64 MPa, showed an increase with clay content up to 8 wt % (1004.61 MPa), but afterward a decrease in modulus value was observed. Toughness of the hybrid materials initially increases but then a decrease is observed with higher amount of organoclay. Chemically linking the polymer chains with layered silicates provided reinforcement to hybrid materials. However, for a given molecular weight of the polymer, there are a particular number of end-groups, which can be linked to the *p*-PDA intercalated clay. If the clay content is increased above 8 wt % it seems that the excess clay platelets may not be linked with polymer chains so the mechanical properties of hybrids deteriorate after further addition of the nanolayers.

Thermogravimetric analysis

Thermal behavior of the polyamide/*p*-PDA-MMT hybrid materials obtained under inert atmosphere at a heating rate of 10°C/min is shown in Figure 4. Thermal decomposition temperatures of the composite samples were found in the range 400–450°C. Decomposition started around 300°C giving some volatiles, followed by maximum weight loss at 450°C. TGA results indicated that these materials were thermally stable that slightly increased with the addition of clay content in the polyamide matrix. The weight retained at 800°C is roughly proportional to the amount of organoclay in the nanocomposites. Incorporation of silicate layers was found to increase the thermal stability presumably due to superior insulating features of the layered silicate which also acts as mass transport barrier to the volatile products generated during decomposition.

Differential scanning calorimetry

The thermal transitions of neat polyamide and nanocomposites were studied using DSC technique, which determined the glass transition temperature of the polymeric materials. The glass transition temperature data for polyamide/*p*-PDA-MMT nanocomposites are given in Table I. These results described a systematic increase in the T_g values with the increase of organoclay contents (Fig. 5), which showed a greater interaction between the two disparate phases. The results of polyamide/organoclay hybrids gave maximum T_g value at 87.6°C with 16 wt % addition of organoclay and then slightly decreased with 20 wt % clay content because entire organoclay may not interact with the polymer matrix resulting in poor interfacial interactions. Incorporation of *p*-PDA-MMT in the matrix restricted the segmental motion of the polymer chains. When the amount of organoclay increased in the nanocomposites, the T_g values shifted toward higher temperature. This suggested that more polyamide chains had linked with organically modified silicate layers. Consequently, the motion of polymer chains was restricted, thereby, increasing the T_g values of the composite materials.

TABLE I
Mechanical, Glass Transition Temperatures, and Water Absorption Data of Aromatic–Aliphatic Polyamide/*p*-PDA-MMT Hybrid Materials

p-PDA-MMT Contents (%)	Maximum stress (MPa)	Maximum strain	Initial modulus (MPa)	Toughness (MPa)	T_g (°C)	Water absorption at equilibrium (%)
0.0	18.86	0.164	386.64	2.629	72.34	16.1
2.0	25.47	0.148	563.90	3.116	–	15.2
4.0	27.03	0.121	666.66	2.636	74.23	14.8
6.0	27.23	0.078	692.80	1.761	–	14.2
8.0	27.50	0.076	1004.61	1.726	76.37	13.9
10.0	25.29	0.065	932.85	1.352	–	13.2
12.0	24.13	0.062	889.75	1.167	79.59	12.9
14.0	23.19	0.052	786.41	0.865	–	12.6
16.0	22.61	0.049	726.71	0.780	87.60	9.2
20.0	22.02	0.033	631.89	0.389	87.54	6.6

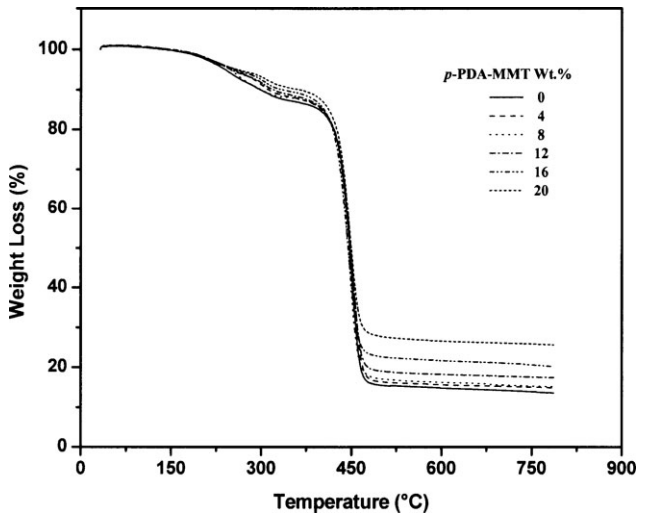

Figure 4 TGA curves of aromatic–aliphatic polyamide/*p*-PDA-MMT nanocomposites obtained at a heating rate of 10°C/min in nitrogen.

Water uptake measurements

Water uptake studies are important for polyamide and its hybrids because of polar groups which have a tendency to absorb water through hydrogen bonding and can badly affect the mechanical and dielectric properties of these nanocomposites. Water uptake data for the composite materials under saturated conditions are given in Table I. The results showed maximum water absorption for the neat polyamide (16.1%) after 168 h, with a decrease thereafter. It is due to the exposure of polar groups to the surface of polymer in which water molecules develop secondary bond forces with these groups. Increase in weight of the films due to water absorption gradually decreases as the clay content in the films increased. The clay platelets obviously restrict the access of water to the hydrogen-bonding sites on the polymer chains. The mutual interaction between the organic and inorganic phases results in lesser availability of polar groups to interact with water. Second, the impermeable clay layers mandate a tortuous pathway for a permeant to transverse the nanocomposite. The improved barrier properties, chemical resistance, reduced solvent uptake, and flame retardance of clay–polymer nanocomposites all result from the hindered diffusion pathways through the nanocomposite.

Structure–property relationship

Polyamide synthesized from the monomers was found to be a good matrix for nanocomposites formation in terms of mechanical and thermal properties. The morphology determined from XRD and TEM revealed both delaminated and intercalated nanocomposites. The nanostructures from intercalated to exfoliated depend on the degree of penetration of polymer chains into the silicate galleries. Polymer intercalation depends on the existence of polar interactions between the organoclay and polymer matrix. Polyamides possess polar amide groups in their backbone and when mixed with organoclay yield disordered and ordered nanostructures. Maximum stress increased relative to the pure polyamide matrix. The organic phase generally has a large free volume and low T_g cannot withstand high stresses but can exhibit very large strain. On the other hand, inorganic ceramic phase which generally has a small free volume and high T_g has the capability of tolerating large stresses but only small strains. The stress is much more efficiently transferred from the polymer matrix to the inorganic filler, resulting in a higher increase in tensile properties. The chemical bonding and enhanced *d*-spacing of silicate layers give more uniform dispersion of the organoclay resulting better tensile properties. The tensile modulus of a polymeric material has been shown to be remarkably improved due to the strong interaction between matrix and silicate layer via formation of hydrogen and chemical bonding. The extent of improvement of modulus depends directly on the average length of dispersed clay particles and hence the aspect ratio. The decease in elongation at break for nanocomposites may be attributed to the presence of some stacks of silicate layers, which

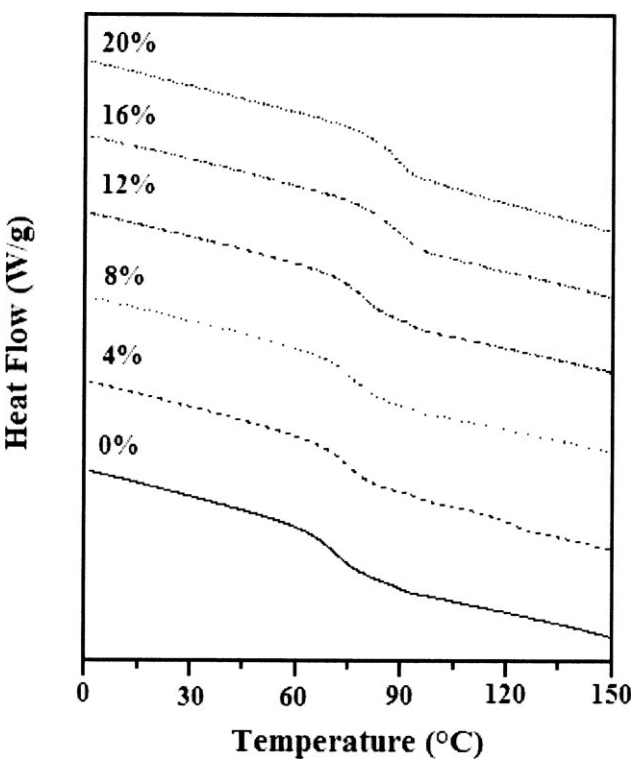

Figure 5 DSC curves of aromatic–aliphatic polyamide/*p*-PDA-MMT nanocomposites.

subsequently decreases the toughness behavior as well. Glass transition temperatures of nanocomposites increased as compared with pure polyamide matrix. This behavior may be explained due to the intercalation of polymer chains into the clay galleries impeding mobility of the polymer segments near the interface.

CONCLUSIONS

Organoclay when added to the polyamide matrix reinforces material with improved compatibility between the two phases. Chemical interaction developed between the organic and inorganic phases yield homogenously dispersed organoclay throughout the matrix. At low concentration particularly up to 8 wt % *p*-PDA-MMT, the dispersion of individual silicate sheet is optimum. When clay increment increases beyond certain limit, it exists in the form of tactoids; which has less cohesion with organic phase and causes adverse effects on the mechanical properties. As the concentration of clay increases, the layers may stack together and intergallery space does not increase much so that more chains can travel into space between the layers. These large size particles then degrade the properties of composites.

Sonia Zulfiqar is grateful to HEC for awarding her fellowship under "International Research Support Initiative Program" (IRSIP) to pursue research work at Max Planck Institute for Polymer Research (MPI-P), Mainz, Germany. Special thanks are due to Prof. Dr. Gerhard Wegner, Director, MPI-P for providing the characterization facilities for the completion of this work.

References

1. Theng, B. K. G. Formation and Properties of Clay-Polymer Complexes. Developments in Soil Science; Elsevier: Amsterdam, 1979.
2. Ogata, N.; Jimenez, G.; Kawai, H.; Ogihara, T. J Polym Sci Part B: Polym Phys 1997, 35, 389.
3. Usuki, A.; Kojima, Y.; Kawasumi, M.; Okada, A.; Fukushima, Y.; Kurauchi, T. J Mater Res 1993, 8, 1179.
4. Kawasumi, M.; Hasegawa, N.; Kato, M.; Usuki, A.; Okada, A. Macromolecules 1997, 30, 6333.
5. Liu, X.; Wu, Q.; Berglund, L. A.; Lindberg, H.; Fan, J.; Qi, Z. J Appl Polym Sci 2003, 88, 953.
6. Liu, X.; Wu, Q. Macromol Mater Eng 2002, 287, 180.
7. Zulfiqar, S.; Sarwar, M. I. Scripta Mater 2008, 59, 436.
8. Zhang, G.; Li, Y.; Yan, D. Polym Int 2003, 52, 795.
9. Zulfiqar, S.; Ishaq, M.; Sarwar, M. I. Surf Interface Anal 2008, 40, 1195.
10. Varlot, K.; Reynaud, E.; Kloppfer, M. H.; Vigier, G.; Varlet, J. J Polym Sci Part B: Polym Phys 2001, 39, 1360.
11. Zulfiqar, S.; Lieberwirth, I.; Ahmad, Z.; Sarwar, M. I. Polym Eng Sci 2008, 48, 1624.
12. Masenelli-Varlot, K.; Reynaud, E.; Vigier, G.; Varlet, J. J Polym Sci Part B: Polym Phys 2002, 40, 272.
13. Zulfiqar, S.; Lieberwirth, I.; Ahmad, Z.; Sarwar, M. I. J Mater Res 2008, 23, 2296.
14. Kojima, Y.; Usuki, A.; Kawasumi, M.; Okada, A.; Kurauchi, T.; Kamigaito, O. J Polym Sci Part B: Polym Phys 1995, 33, 1039.
15. Kojima, Y.; Usuki, A.; Kawasumi, M.; Okada, A.; Kurauchi, T.; Kamigaito, O. J Polym Sci Part A: Polym Chem 1993, 31, 1755.
16. Liu, L.; Qi, Z.; Zhu, X. J Appl Polym Sci 1999, 71, 1133.
17. Wu, T. M.; Hsu, S. F.; Wu, J. Y. J Polym Sci Part B: Polym Phys 2002, 40, 736.
18. Chen, G. H.; Wu, D. J.; Weng, W. G.; He, B.; Yan, W. Polym Int 2001, 50, 980.
19. Kim, T. H.; Lim, S. T.; Lee, C. H.; Choi, H. J.; Jhon, M. S. J Appl Polym Sci 2003, 87, 2106.
20. Tseng, C. R.; Wu, S. C.; Wu, J. J.; Chang, F. C. J Appl Polym Sci 2002, 86, 2492.
21. Kim, T. H.; Jang, L. W.; Lee, D. C.; Choi, H. J.; Jhon, M. S. Macromol Rapid Commun 2002, 23, 191.
22. Tseng, C. R.; Lee, H. Y.; Chang, F. C. J Polym Sci Part B: Polym Phys 2002, 39, 2097.
23. Tang, Y.; Hu, Y.; Wang, S.; Gui, Z.; Chen, Z.; Fan, Z. Polym Int 2003, 52, 1396.
24. Zhang, Q.; Fu, Q.; Jiang, L.; Lei, Y. Polym Int 2000, 49, 1561.
25. Koo, C. M.; Kim, M. J.; Choi, M. H.; Kim, S. O.; Chung, I. J. J Appl Polym Sci 2003, 88, 1526.
26. Xu, W.; Ge, M.; He, P. J Polym Sci Part B: Polym Phys 2002, 8, 408.
27. Jin, Y.-H.; Park, H.-J.; Im, S.-S.; Kwak, S.-Y.; Kwak, S. Macromol Rapid Commun 2002, 23, 135–140.
28. Alexandre, M.; Dubois, P.; Sun, T.; Graces, J. M.; Jerome, R. Polymer 2002, 43, 2123.
29. Okamoto, M.; Morita, S.; Kotaka, T. Polymer 2001, 42, 2685.
30. Okamoto, M.; Morita, S.; Kim, Y. H.; Kotaka, T.; Tateyama, H. Polymer 2001, 42, 1201.
31. Hyun, Y. H.; Lim, S. T.; Choi, H. J.; Jhon, M. S. Macromolecules 2001, 34, 8084.
32. Lim, S. K.; Kim, J. W.; Chin, I.; Kwon, Y. K.; Choi, H. J. Chem Mater 2002, 14, 1989.
33. Kornmann, X.; Thomann, R.; Mulhaupt, R.; Finter, J.; Berglund, L. A. Polym Eng Sci 2002, 42, 1815.
34. Becker, O.; Varley, R.; Simon, G. Polymer 2002, 43, 4365.
35. Zulfiqar, S.; Ahmad, Z.; Ishaq, M.; Saeed, S.; Sarwar, M. I. J Mater Sci 2007, 42, 93.
36. Kausar, A.; Zulfiqar, S.; Shabbir, S.; Ishaq, M.; Sarwar, M. I. Polym Bull 2007, 59, 457.
37. Bibi, N.; Sarwar, M. I.; Ishaq, M.; Ahmad, Z. Polym Polym Compos 2007, 15, 313.
38. Zulfiqar, S.; Ahmad, Z.; Sarwar, M. I. Colloid Polym Sci 2007, 285, 1749.
39. Zulfiqar, S.; Lieberwirth, I.; Sarwar, M. I. Chem Phys 2008, 344, 202.
40. Zulfiqar, S.; Ishaq, M.; Ahmad, Z.; Sarwar, M. I. Polym Adv Technol 2008, 19, 1250.
41. Zulfiqar, S.; Sarwar, M. I. High Perform. Polymers 2009, Online First (DOI:10.1177/0954008308089114).
42. Sarwar, M. I.; Zulfiqar, S.; Ahmad, Z. Colloid Polym Sci 2007, 285, 1733.
43. Sarwar, M. I.; Zulfiqar, S.; Ahmad, Z. J. Sol-Gel Sci Technol 2008, 45, 89.
44. Sarwar, M. I.; Zulfiqar, S.; Ahmad, Z. J Sol Gel Sci Technol 2007, 44, 41.
45. Sarwar, M. I.; Zulfiqar, S.; Ahmad, Z. Polym Int 2008, 57, 292.
46. Sarwar, M. I.; Zulfiqar, S.; Ahmad, Z. Polym Compos 2009, 30, 95.
47. Maiti, P.; Nam, P.H.; Okamoto, M.; Hasegawa, N.; Usuki A. Macromolecules 2002, 35, 2042.